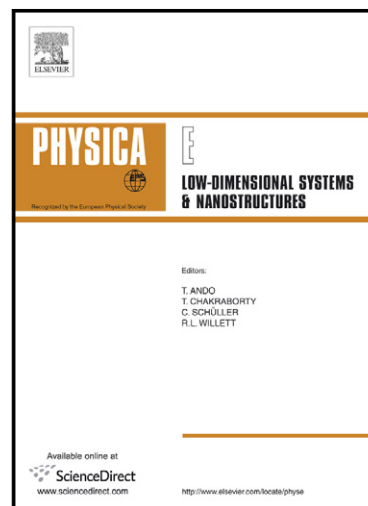


Temperature- dependent electrical transport properties of (Au/Ni) n-GaN Schottky barrier diodes

Hulya Dogan, Sezai Elagoz



www.elsevier.com/locate/physa

PII: S1386-9477(14)00146-5
DOI: <http://dx.doi.org/10.1016/j.physe.2014.04.019>
Reference: PHYSE11587

To appear in: *Physica E*

Received date: 12 November 2013

Revised date: 16 April 2014

Accepted date: 22 April 2014

Cite this article as: Hulya Dogan, Sezai Elagoz, Temperature- dependent electrical transport properties of (Au/Ni) n-GaN Schottky barrier diodes, *Physica E*, <http://dx.doi.org/10.1016/j.physe.2014.04.019>

This is a PDF file of an unedited manuscript that has been accepted for publication. As a service to our customers we are providing this early version of the manuscript. The manuscript will undergo copyediting, typesetting, and review of the resulting galley proof before it is published in its final citable form. Please note that during the production process errors may be discovered which could affect the content, and all legal disclaimers that apply to the journal pertain.

Temperature- dependent electrical transport properties of (Au/Ni) n-GaN Schottky barrier diodes.

Hulya Dogan^(a), Sezai Elagoz^{(b),(c)}

^(a) Department of Electrical-Electronics Engineering, Cumhuriyet University , Sivas 58140, Turkey , *hdogan@cumhuriyet.edu.tr*

^(b) Department of Nanotechnology Engineering, Cumhuriyet University, Sivas 58140, Turkey

^(c) Nanotechnology Research Center, Cumhuriyet University, Sivas 58140, Turkey, *elagoz@cumhuriyet.edu.tr*

Abstract

The temperature-dependent electrical properties of (Au/Ni)/n-GaN Schottky barrier diodes (SBDs) have been investigated in the wide temperature range of 40-400 K. The analysis of the main electrical characteristics such as zero-bias barrier height (Φ_{B0}), ideality factor (n) and series resistance (R_s) were found strongly temperature dependent. Such behaviour is attributed to barrier inhomogeneities by assuming a Gaussian distribution (GD) of barrier heights (BHs) at the interface. It is evident that the diode parameters such as zero-bias barrier height increases and the ideality factor decreases with increasing temperature. The values of series resistance that are obtained from Cheung's method is decreasing with increasing temperature. The temperature dependence of Schottky barrier height (SBD) and ideality factor (n) are explained by invoking three sets of Gaussian distribution of (SBH) in the temperature ranges of 280-400 K, 120-260 K and 40-100 K, respectively. (Au/Ni)/n-GaN Schottky barrier diode have been shown a Gaussian distribution giving mean BHs ($\bar{\Phi}_{B0}$) of 1.167, 0.652 and 0.356 eV and standard deviation σ_s of 0.178, 0.087 and 0.133 V for the three temperature regions. A modified $\ln(I_0/T^2) - q^2\sigma^2/2k^2T^2$ vs. $1/kT$ plot have given $\bar{\Phi}_{B0}$ and A^* as 1.173 eV and 34.750 A/cm² K², 0.671 eV and 26.293 A/cm² K², 0.354 eV and 10.199 A/cm² K², respectively.

1. Introduction

Group III nitride wide band gap semiconductors have attracted considerable interest owing to their applications for optical devices operating in the blue and ultraviolet wavelength regions. These materials and especially gallium nitride (GaN), were also found to be suitable for operation at high electrical and optical power levels, high temperatures and in harsh environments [1-6]. The electrical characteristics of the GaN devices under these different temperature conditions are essential. The ideality factor n and more especially the barrier height Φ_B are the most important characteristics of metal-semiconductor Schottky barrier contacts. Nevertheless, obtaining reproducible rectifying contacts on GaN with a high and ideal Schottky barrier Φ_B and a low leakage current still remains a serious technological concern, whose physical origin is continuously object of investigation. Typically, metals with a high work function (such as Pt, Ni, and Pd) are used for Schottky contacts to n -type GaN since, according to the Schottky-Mott [17] relation, they are expected to give high Schottky barrier height values. Schottky metallizations for n -GaN are based on Au/Ni, the thin films as such Au are generally used as a top layer to reduce the sheet resistance of the contact and to protect the other metallic layers from the oxidation and against other adverse effects[44].

GaN and related compounds have been studied extensively for applications in short wavelength optical devices (LEDs) [7], heterostructure transistors (HFETs), metal semiconductor field effect transistors (MESFETs), high electron mobility transistor (HEMTs) and rectifiers[8-10].

Temperature dependent I - V characteristics of metal Schottky contacts on n -GaN have been studied by many researchers in different temperature ranges. Dogan et al. [11] performed measurements on Au/Ni/ n -GaN Schottky contacts in the 40-320 K temperature range. Their results indicate the variation in the I - V characteristics in three different regions, with thermionic emission being the dominant transport mechanism. From their report, they revealed the variation of the Richardson constant within these regions. Lakshmi et al. [12] also studied the I - V characteristics of Au/ n -GaN (MIS) Schottky contacts in the 120-390 K temperature range while Reddy et al. [13] studied the I - V characteristics of the Ni/Pd/ n -GaN Schottky contacts in the 100-425 K temperature range. In all their reports, they have reported

the dependence of the barrier height and ideality factor on temperature. Demirezen et al. [14] studied the current-voltage-temperature (I-V-T) characteristics of inhomogeneous (Ni/Au)- $\text{Al}_{0.22}\text{Ga}_{0.78}\text{N}/\text{AlN}/\text{GaN}$ heterostructures in the temperature range 80-400K. They reported that the R_s plays a crucial role in affecting the forward bias I-V curves of SBDs. The values of R_s show an unusual behaviour, in which it increases with an increase of temperature. Peta et al. [15] studied I-V characteristics of (Pt/Au)/ Ga-polarity GaN/Si (111) Schottky diode in the 200-375 K temperature range. They reported that Φ_{B0} , n and R_s are strongly temperature dependent.

In this work, an attempt is made to investigate the detailed electrical properties of (Au/Ni)/ n -GaN Schottky barrier diodes (SBDs) in a wide temperature range 40-400 K with a temperature step of 20 K by using the forward bias I-V measurements. Barrier height (Φ_{B0}), ideality factor (n) and series resistance (R_s) of the device are extracted from the forward bias I-V measurements. The series resistance (R_s) parameter determined from forward bias I-V characteristics using Cheung and Cheung's method [16]. It has been seen an increase in ideality factor and decrease in apparent barrier height, and significant deviations from linearity in the Richardson plots with a decrease in temperature for diode. The temperature dependence of SBH characteristics of (Au/Ni)/ n -GaN SBD was interpreted on the basis of the existence of three Gaussian distributions of the barrier heights (BH) around a mean value due to barrier height inhomogeneities prevailing at the M/S interface.

2. Experimental details

The n -GaN films used in this study were epitaxially grown by metal organic chemical vapor deposition (MOCVD) on c-plane Al_2O_3 substrates. An undoped GaN layer thickness of 1250 nm was grown followed by the growth of 1350 nm thick n -GaN: Si ($N_d = 1.01 \times 10^{18} \text{ cm}^{-3}$) layer. The n -GaN was first ultrasonically cleaned with methanol followed by acetone and trichloroethylene for 5 min each. For the contacts, since the sapphire substrate is insulating, the ohmic and Schottky contacts were made on the top surface. The ohmic contacts were prepared by the evaporation deposition of Ti (90 nm)/Au (thermal evaporation). After the metallization step, the contacts were annealed at 650 °C for 3 min in N_2 ambient in order to form the ohmic contact. The Schottky contacts were prepared by the evaporation deposition of Au (thermal evaporation)/Ni (70 nm). Ni (70 nm) Schottky contacts were made using magnetron DC sputter technique and Au (thermal evaporation) as a top layer to protect Ni metallic layer was evaporated onto Ni/ n -GaAs structure in high vacuum system of 10^{-6} Torr.

Both ohmic and Schottky contacts were made on the top surface as 1.5-mm-diameter circular dots (see Fig. 1). The I-V characteristics of the devices were measured using a Keithley 487 Picoammeter/Voltage Source in the temperature range of 40-400 K by means of a temperature controlled ARS HC-2 closed-cycle helium cryostat which enables us to make measurements in the temperature range of 20-450 K under dark conditions.

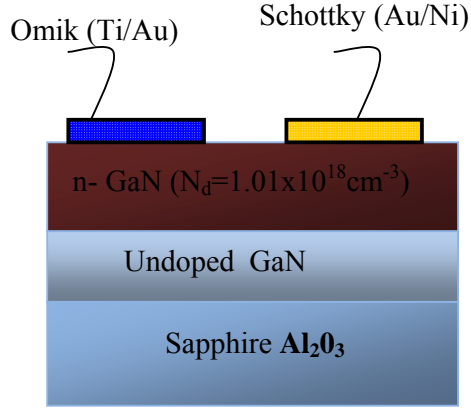


Fig. 1. Schottky contact on n-GaN

3. Results and discussion

3.1. Analysis of current-voltage-temperature (I-V-T) characteristics

The current through a (Au/Ni)/n-GaN SBD with the R_s in the forward bias, based on the thermionic emission (TE) theory, is given by the relation [17]

$$I = I_0 \exp\left(\frac{q(V - IR_s)}{nkT}\right) \left[1 - \exp\left(\frac{-q(V - IR_s)}{kT}\right) \right] \quad (1)$$

where I_0 is the saturation current defined by

$$I_0 = AA^*T^2 \exp\left(-\frac{q\Phi_{B0}}{kT}\right) \quad (2)$$

Φ_{B0} is the zero bias apparent barrier height (BH), q is the electron charge, k is the Boltzmann constant, T is the absolute temperature, V is the forward-bias voltage, A is the effective diode area, A^* is the Richardson constant and equal to $26.4 \text{ A cm}^{-2} \text{ K}^{-2}$ for n -type GaN [18]. R_s is the

series resistance of the neutral region of the semiconductor bulk (between the depletion region and ohmic contact), IR_s is the voltage drop across the series resistance. The ideality factor n and the Φ_{B0} can be written as accounts for the departure of the current transport mechanisms from the ideal TE model using the definition:

$$n = \frac{q}{kT} \left(\frac{dV}{d \ln I} \right) \quad (3)$$

$$\Phi_{B0} = \frac{kT}{q} \ln \left(\frac{AA^*T^2}{I_0} \right) \quad (4)$$

The forward bias I - V characteristics of the Au/Ni/ n -GaN Schottky diodes were measured in the temperature range of 40-400 K with steps of 20 K. Fig. 2 shows the temperature dependence of the I - V characteristics under forwards bias. These I - V plots shift towards the higher bias side with decrease in temperature. The high voltage regime was assumed to be due to some mechanisms other than thermionic emission. For example, the recombination current become dominant under these conditions [19] and at larger forward bias, the series resistance leads to the deviation from the straight line [20]. In the I - V plots for all measurement temperature at low-voltage, the ideality factor and the Φ_{B0} can be obtained by the thermionic emission theory.

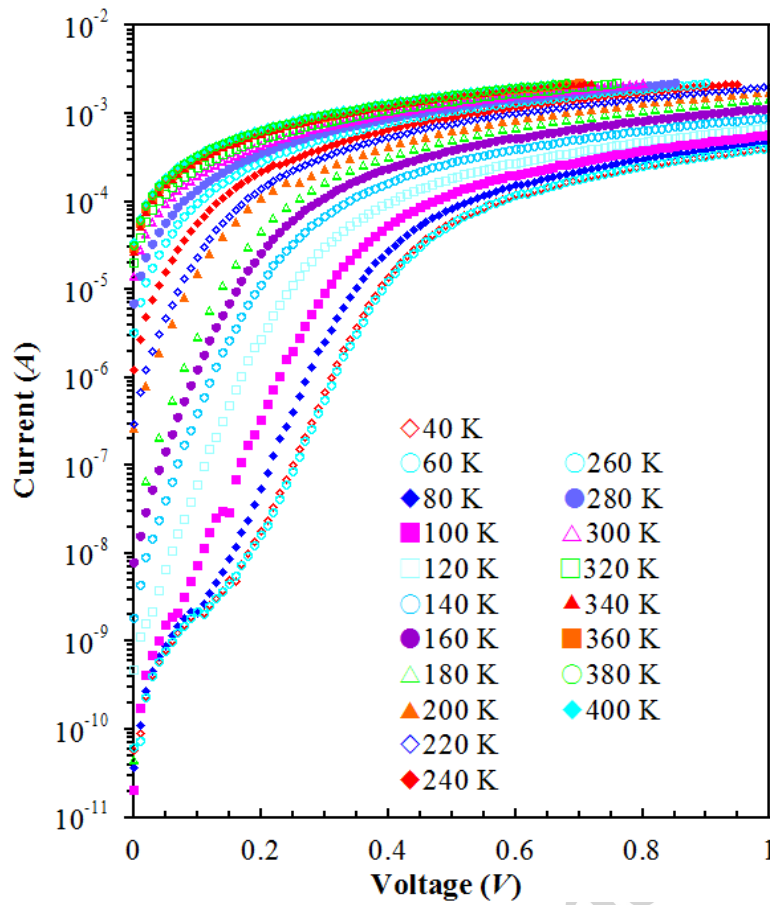


Fig. 2. Forward bias semi-logarithmic I-V characteristics of (Au/Ni)/n-GaN SBD at various temperatures.

The temperature dependent values of zero-bias apparent SBH ($\Phi_{B0} = \Phi_{ap}$) and apparent n_{ap} are obtained from Eqs. (3) and (4), respectively, and are given in Table 1, Fig. 3 and 4. As shown in Table 1, the values of Φ_{B0} and n for the (Au/Ni)/n-GaN SBD ranged from 0.110 eV and 7.85 (at 40 K) to 0.721 eV and 1.289 (at 400 K), respectively. The large value of n has been attributed to the presence of interface states and barrier inhomogeneity at metal-semiconductor interface [17, 21, 22].

Table 1

Temperature dependent values of various parameters determined from forward bias I–V characteristics of (Au/Ni)/*n*-GaN SBD.

T(K)	$n_{(I-V)}$	$\Phi_{Bo(I-V)} (eV)$	$\Phi_{Bo(H-I)} (eV)$	$R_{s(dV/d(\ln I))} (\Omega)$	$R_{s(H-I)} (\Omega)$
40	7.850	0.110	0.104	1217.76	1287.61
60	5.225	0.170	0.143	1188.56	1213.88
80	3.777	0.223	0.187	1079.33	1098.56
100	2.959	0.269	0.205	919.53	904.60
120	2.556	0.301	0.264	866.02	882.81
140	2.273	0.332	0.299	724.42	733.53
160	2.085	0.368	0.340	598.55	607.80
180	1.925	0.403	0.374	480.44	489.18
200	1.823	0.419	0.388	409.10	425.20
220	1.727	0.454	0.403	361.25	360.06
240	1.649	0.475	0.439	331.13	338.26
260	1.573	0.497	0.433	298.58	289.57
280	1.520	0.526	0.481	310.92	317.32
300	1.476	0.549	0.488	292.95	291.70
320	1.419	0.582	0.519	287.68	289.02
340	1.384	0.614	0.543	286.90	285.11
360	1.340	0.650	0.572	282.97	278.23
380	1.321	0.685	0.599	274.82	266.28
400	1.289	0.721	0.638	267.30	247.57

Since the current transport across the M/S interface is a temperature activated process, the electrons at low temperatures are able to surmount the lower barriers [23-25]. Therefore, the current transport will be dominated by the current flowing through the patches of lower SBH, leading to a larger ideality factor. In addition, as shown in Fig. 3 and 4, there are three linear regions. The three temperature regions have given for 280-400 K range (the distribution 1), 120-260 K range (the distribution 2), and 40-100 K range (the distribution 3).

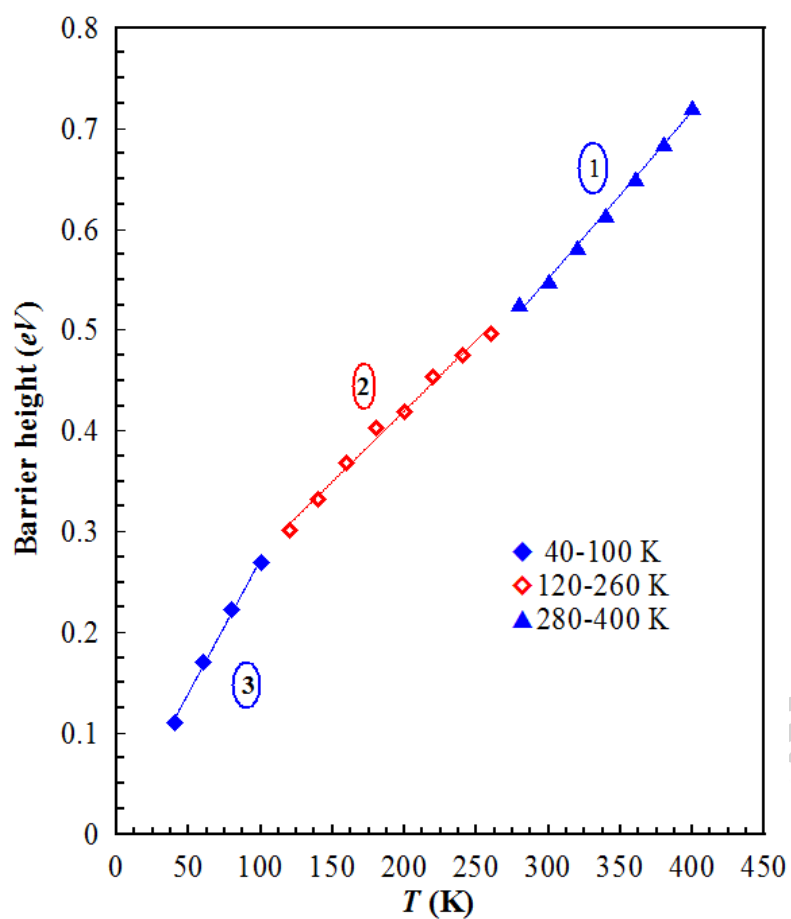


Fig. 3. The temperature dependence of BH for (Au/Ni)/n-GaN SBD obtained from the forward bias I - V data at various temperatures.

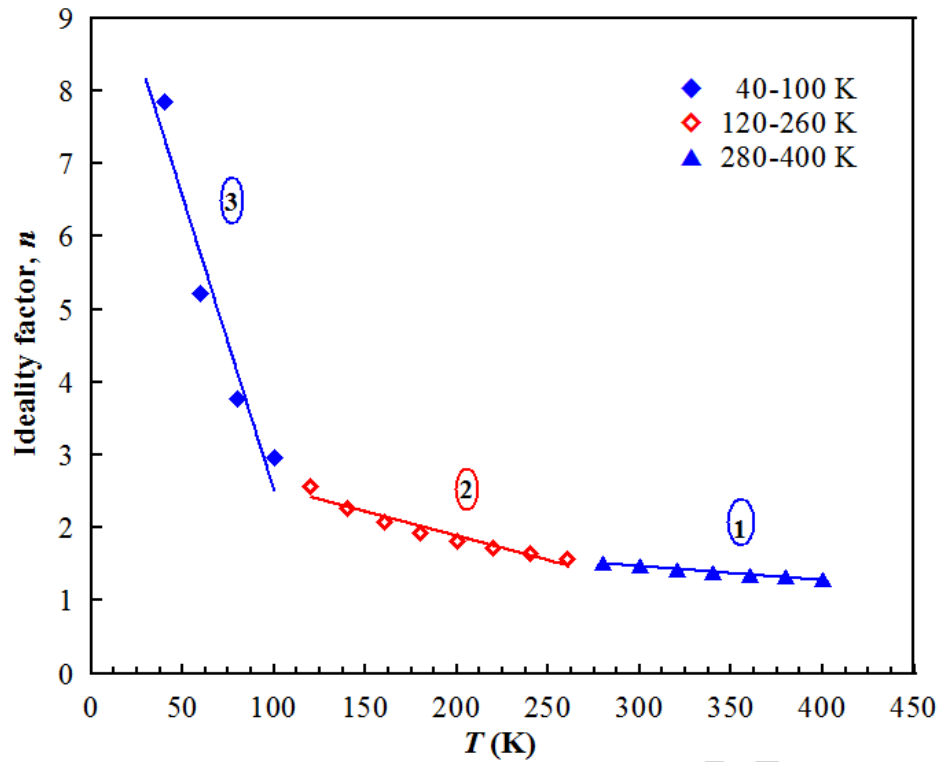


Fig. 4. The temperature dependence of n for (Au/Ni)/n-GaN SBD obtained from the forward bias I - V data at various temperatures.

The series resistance plays an important role in determining the electrical parameter of the Schottky diode because it limits the conduction process particularly in large band gap semiconductor materials such as GaN. The resistance of the Schottky diode is the sum of total resistance value of the resistors in series resistance in semiconductor device in the direction of current flow. The R_s are evaluated from the forward bias I - V data using methods developed by Cheung and Cheung method [16]. The temperature dependence of the R_s values is given in Fig. 5. As shown from Fig. 5, the value of R_s decreases strongly with increasing temperature. Table 1 shows the barrier height, ideality factor and series resistance values determined from the Cheung's equations, for each temperature. As shown in Table 1, the obtained Φ_B and R_s values by different techniques are in good agreement with each other. The decrease of R_s with the increasing temperature could be due to the factors responsible for increase of ideality factor and lack of free carrier concentration at low temperatures [26].

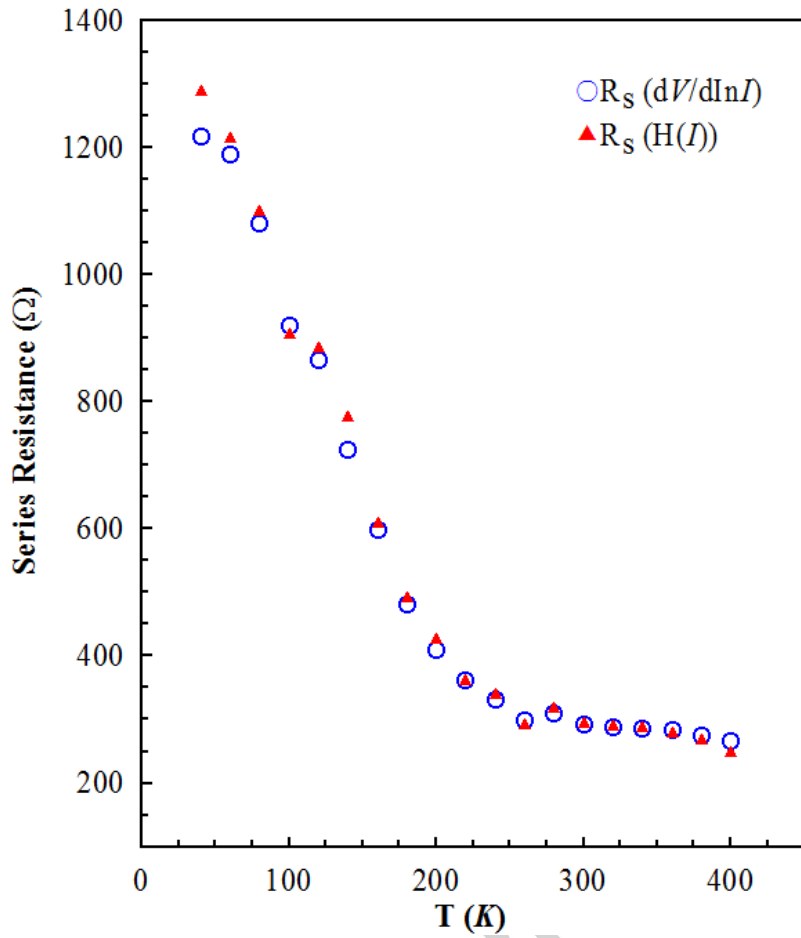


Fig.5. The temperature dependence of the series resistances obtained from Cheung's method for (Au/Ni)/n-GaN SBD.

3.2 Inhomogeneous barrier analysis

For the evaluation of the BH, one may also make use of conventional Richardson plot of the reverse saturation current. Eq. (2) can be written as

$$\ln\left(\frac{I_0}{T^2}\right) = \ln(AA^*) - \frac{q\Phi_{B0}}{kT} \quad (5)$$

The temperature dependence of experimental $\ln(I_0/T^2)$ vs. $10^3/T$ was found to be non-linear in the measured temperature range. However, the dependence of $\ln(I_0/T^2)$ vs. $10^3/nT$ plot gives a straight line (Fig. 6). The experimental data are seen to fit asymptotically to a linear region in the studied temperature range of 40- 400 K. The values of the activation energy (E_a) and Richardson constant (A^*) were obtained from the slope and intercept of this straight line as 0.732 eV and $2.05 \text{ Acm}^{-2}\text{K}^{-2}$, respectively. However, the $\ln(I_0/T^2)$ vs. $10^3/T$ plot is not linear below 140 K due to strong temperature dependence of Φ_{B0} and n [27-29]. The effective Richardson constant and BH values can be determined from linear part of $\ln(I_0/T^2)$ vs. $10^3/T$ plot at high temperature region. The values of the E_a at 0 K was calculated as 0.133 eV from

the slope of the plot and (A^*) was found to be $1.722 \times 10^{-6} \text{ A cm}^{-2} \text{ K}^{-2}$ from y-axis intercept of the plot. This value of A^* in (Au/Ni)/n-GaN SBD is much lower than the theoretical value of $26.4 \text{ A cm}^{-2} \text{ K}^{-2}$. The deviation in the Richardson plots may be due to the spatial inhomogeneous barrier height and potential fluctuations at the interface that consist of low and high barrier areas [23, 26, 30, 31]. That is, the current through the diode will flow preferentially through the lower barriers in the potential distribution.

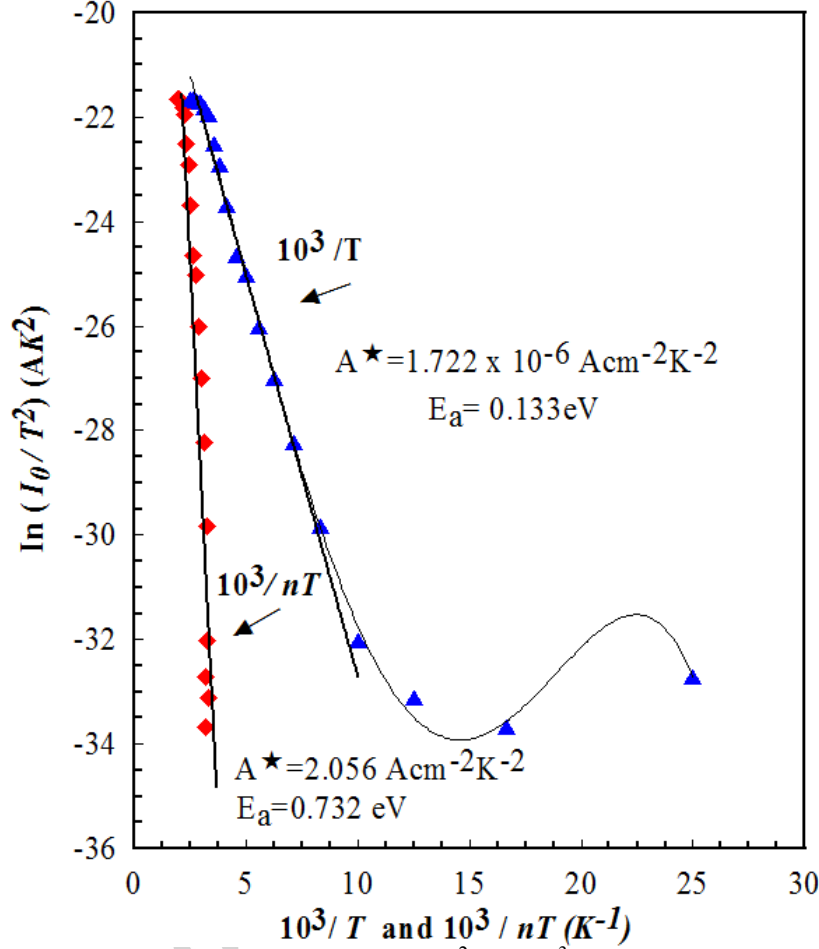


Fig.6. Richardson plots of the $\ln(I_0/T^2)$ vs. $10^3/nT$ for (Au/Ni)/n-GaN SBD.

Fig. 7 shows a plot of the experimental BH vs. the n . As can be seen from Fig. 7, the BHs become smaller as the ideality factors increase. That is, there is a linear relationship between the experimental effective BHs and ideality factors of the (Au/Ni)/n-GaN Schottky diode. This finding may be attributed to lateral barrier inhomogeneities of Schottky diodes [32-37] be seen in Fig. 7, there are three linear regions between Φ_{B0} and n values of the (Ni/Au)/n-GaN SBD, which can be explained by the lateral inhomogeneities of the barrier heights [21]. In the first region (280–400 K), the extrapolation of the experimental Φ_{B0} and n plot to $n = 1$ has given the value of 0.945 eV. In the second region (120–260 K), the extrapolation of the Φ_{B0} and n plot to $n = 1$ has given the value of 0.597 eV. In the third region (40–100 K), the extrapolation of the Φ_{B0} and n plot to $n = 1$ has given the value of 0.317 eV. Thus, it can be

said that the significant decrease of the zero-bias BH and increase of the n especially at low temperature are possibly caused by the BH inhomogeneities.

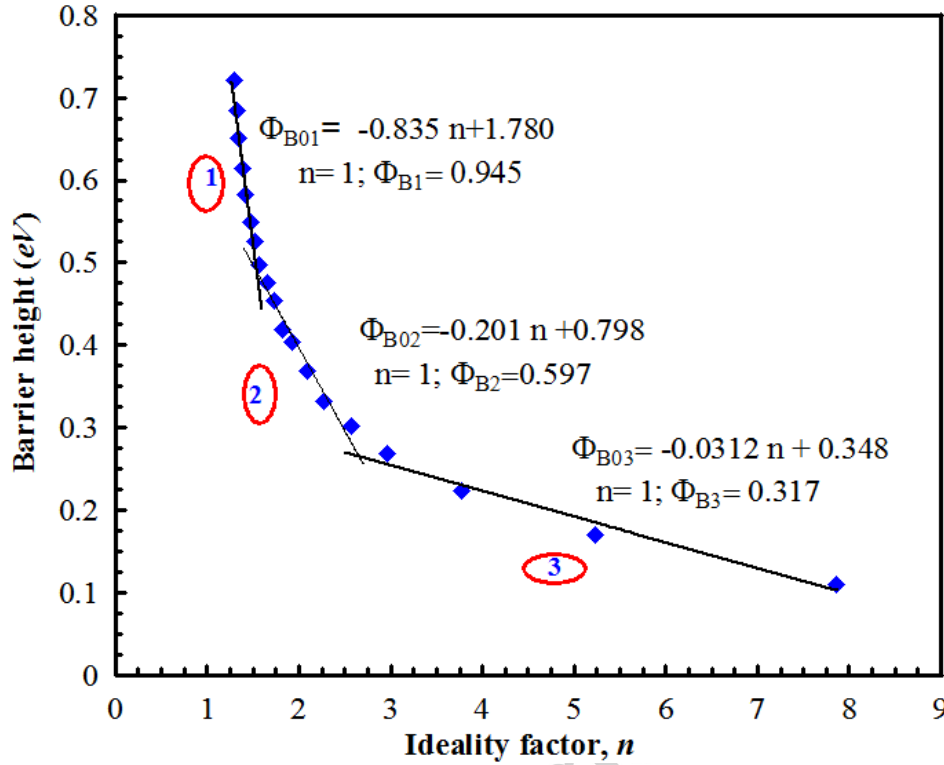


Fig.7. Plot of the experimental BH vs. the n for (Au/Ni)/n-GaN SBD.

According to barrier inhomogeneity model, assume a continuous spatial distribution of the local Schottky barrier patches; and total current across a Schottky diode is obtained by integrating the thermionic current expression with an individual SBH and weighted by using the Gaussian distribution function across all patches. The Gaussian distribution of the apparent barrier height can be written as [24]

$$\Phi_{ap} = \bar{\Phi}_{B0} - q\sigma_{s0}^2 / 2kT \quad (6)$$

where σ_{s0} is the zero bias standard deviation of the BH distribution and it is a measure of the barrier homogeneity. The temperature dependence of σ_{s0} is usually small and can be neglected. Thus SBH has a Gaussian distribution with the zero bias mean SBH, $\bar{\Phi}_{B0}$. The observed variation of ideality factor with temperature in the model is given by [38].

$$-\partial\Phi_{ap} / \partial V = (n_{ap}^{-1} - 1) = -\rho_2 + \rho_3 q / 2kT \quad (7)$$

The voltage-independent ideality factor n requires a linear increase in $\Phi_B(V,T)$ with the bias. This is only possible if the mean SBH Φ_B as well as the square of the standard deviation σ^2 vary linearly with the bias [11, 24, 39,40].

$$\Delta\Phi_B(V, T) = \Phi_B(V, T) - \Phi_B(0, T) = \rho_2 V, \quad (8)$$

$$\Delta\sigma^2(V) = \sigma^2(V) - \sigma^2(0) = \rho_3 V. \quad (9)$$

As can be seen from Eqs. (8) and (9), ρ_2 is the voltage coefficient of the mean SBH, and ρ_3 is the voltage coefficient of the standard deviation. According to Eq. (7), a plot of $(n_{ap}^{-1} - 1)$ against $1/2kT$ should give a straight line with the slope and y-axis intercept related to the voltage coefficients ρ_2 and ρ_3 , respectively. The value of ρ_3 are negative for in the entire temperature ranges, indicating a decrease of σ^2 and thus a more homogeneous SBH with increasing voltage. By contrast, the mean SBH exhibits a positive value of the ρ_2 for 120-260 K range (the distribution 2) and 40-100 K range (the distribution 3), and a negative value for 280-400 K range (the distribution 1). The negative value of ρ_2 corresponds to a decrease of $\bar{\Phi}_B$ with increasing voltage. In the positive value of ρ_2 , the tunneling current preponderant yielding and the $\bar{\Phi}_B$ increases with the voltage.

The experimental Φ_{ap} vs. $1/2kT$ and n_{ap} vs. $1/2kT$ plots (Fig. 8), obtained by means of the data obtained from Fig. 2, respond to three lines instead of a single straight line with transition occurring at 260 and 100 K. Fitting of the experimental I - V data to Eqs. (2) and (3) gives Φ_{ap} and n_{ap} , respectively, which should obey Eqs. (6) and (7). Thus, the plot of Φ_{ap} vs. $1/2kT$ (Fig. 8a) should be a straight line with the intercept at the ordinate determining the zero bias mean BH $\bar{\Phi}_{B0}$ and a slope giving the zero bias standard deviation σ_{s0} .

The linearity of the apparent barrier height or ideality factor vs. $1/2kT$ curves in Fig. 8a and b, and the continuous curves in Fig. 2 and Fig. 8a show that the temperature-dependent experimental data of the (Au/Ni)/ n -GaN Schottky contact are in agreement with the recent model which is the related to thermionic emission over a Gaussian BH distribution [22,23] and [41]. The above observations indicate the presence of three Gaussian distributions of barrier heights in the contact area. When the dots have been considered, the intercept and slope of this straight lines given three sets of values of $\bar{\Phi}_{B0}$ and σ_{s0} as 1.167 eV and 0.178 V in the temperature range 280–400 K (the distribution 1), 0.652 eV and 0.087 V in the temperature range 120–260 K (the distribution 2), and 0.356 eV and 0.133 V in the temperature range 40-100 K (the distribution 3).

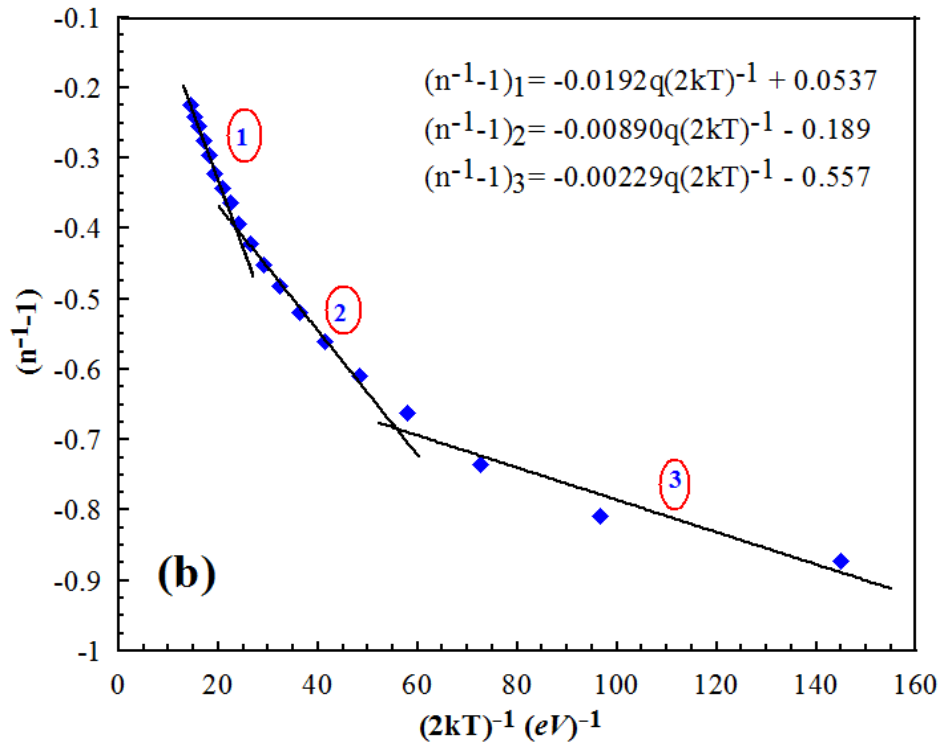
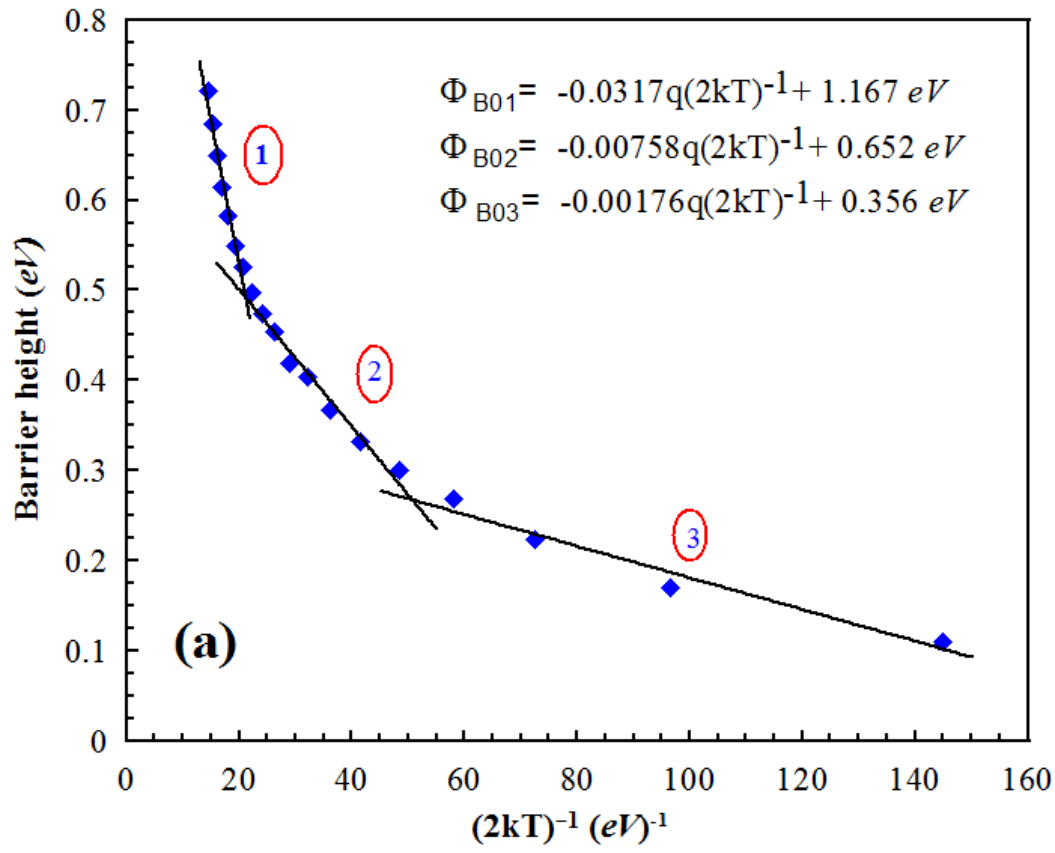


Fig. 8. (a) The zero-bias apparent barrier height ($\Phi_{B0}(I-V)$) vs. $1/2kT$ plot, (b) the ideality factor ($n^{-1}-1$) vs. $1/2kT$ plot for (Au/Ni)/n-GaN SBD according to the three Gaussian distribution.

The existence of a Gaussian in Schottky diodes was already experimentally noted by Ballistic electron emission microscopy (BEEM) [42,43]. Chand and Kumar [30] explained the existence of a Gaussian distribution in the metal/semiconductor contacts that can be attributed to the nature of inhomogeneities themselves. This may involve variation in the interface composition/phase, interface quality, electrical charges, nonstoichiometry, etc. Further, such inhomogeneities might occur on a scale that inhibits their detection by the usual characterization tools. They influence the I-V characteristics of the Schottky diodes at particularly low temperatures. Thus, I-V measurements at very low temperatures are capable of revealing the nature of barrier inhomogeneities present in the contact area. As shown in Fig. 3 (Φ_{B0} vs. T), 4 (n vs. T), 7 (Φ_{B0} vs. n) and 8 [$(n_{ap}^{-1} - 1)$ vs. $1/2kT$], there are three straight lines with different slopes.

Similarly, as can be clearly seen from Fig. 8b, the plot of $(n_{ap}^{-1} - 1)$ vs. $1/2kT$ should also possess different characteristics in the three temperature ranges because the diode contains three barrier height distributions. The values of ρ_2 obtained from the intercepts of the experimental $(n_{ap}^{-1} - 1)$ vs. $1/2kT$ plot are -0.0537 V in 280–400 K range (the distribution 1), 0.189 V in 120–260 K range (the distribution 2) and 0.557 V in 40–100 K range (the distribution 3), where as the values of ρ_3 from the slopes are -0.0192 V in 280–400 K range, -0.0089 V in 120–260 K range and -0.00229 V 40–100 K range. The linear behavior of this plot demonstrates that the n indeed expresses the voltage deformation of the GD of the SBH. The continuous solid lines in Fig. 3 represent data estimated with the above values of ρ_2 and ρ_3 using Eq. (7). As can be seen from the $(n_{ap}^{-1} - 1)$ vs. $1/2kT$, ρ_3 value or the slope of the distribution 1 is larger than the distribution 2 and 3.

As indicated above, the conventional activation energy $\ln(I_0/T^2)$ vs. $1/T$ plot has shown non-linearity at low temperatures. To explain these discrepancies, according to the Gaussian distribution of the BH, we can rewritten as

$$\ln(I_0 / T^2) - (q^2 \sigma_{s0}^2 / 2k^2 T^2) = \ln(AA^*) - q\bar{\Phi}_{B0} / kT \quad (10)$$

and a modified activation energy plot from this expression is obtained. Using the experimental I_0 data, a modified $\ln(I_0/T^2) - q^2 \sigma^2 / 2k^2 T^2$ vs. $1/(kT)$ plot (Fig. 9) can be obtained according to Eq. (10) and should give a straight line with slope directly yielding the mean

Φ_{B0}^* and the intercept ($= \ln AA^*$) at the ordinate determining A^* for a given diode area A . The $\ln(I_0/T^2) - q^2 \sigma^2 / 2k^2 T^2$ values were calculated for both three values of σ_s obtained for the temperature ranges of 280–400 K, 120–260 K, and 40–100K. Thus, Fig. 9 have given the modified $\ln(I_0/T^2) - q^2 \sigma^2 / 2k^2 T^2$ vs. $1/(kT)$ plots for all the three values of σ_s . The best linear fitting to these modified experimental data is depicted by solid lines in Fig. 9 which represent

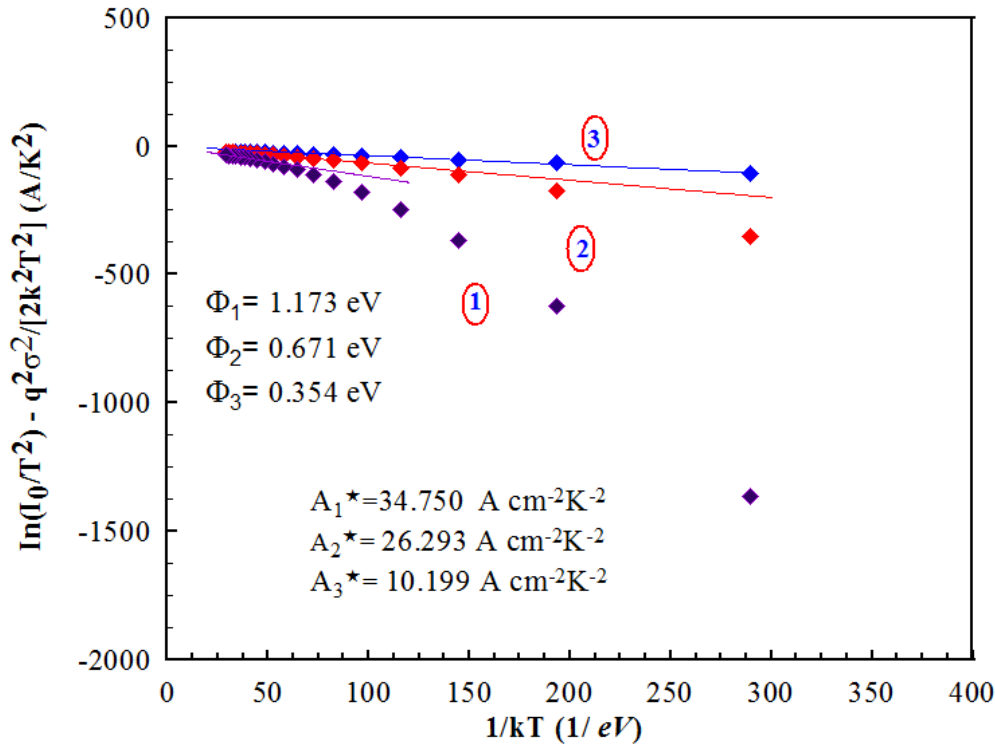


Fig.9. Modified Richardson ($\ln(I_0/T^2) - q^2 \sigma_0^2 / 2k^2 T^2$) plot for (Au/Ni)/n-GaN SBD according to the three Gaussian distributions of the barrier height.

the true activation energy plots in respective temperature ranges. The statistical analysis yielded zero-bias mean BH of 1.173 eV (in the range 280–400 K), 0.671 eV (in the range 120–260 K), and 0.354 eV (in the range 40–100 K). These values match exactly with the mean BHs obtained from the Φ_{ap} vs. $1/(2kT)$ plot in Fig 8a. The interceptions at the ordinate give the Richardson constant A^* as 34.750 A/cm² K² (in 280–400 K range), 26.293 A/cm² K² (in 120–260 K range), and 10.199 A/cm² K² (in 40–100 K range) without using the temperature coefficient of the BHs. This value of the Richardson constant 26.296 A/cm² K² is very close to the theoretical value of 26.4 A/cm² K² for (Au/Ni)/n-GaN.

4. Conclusions

The electrical characteristics of (Au/Ni)/n-GaN Schottky barrier diodes (SBD) have been investigated in a wide temperature range of 40–400 K by using the I - V measurements. It is found that the zero-bias barrier heights (0.110–0.721 eV) increased the ideality factor (7.850–1.289) and series resistance decreased with increasing temperature. Such behaviour is attributed to the Schottky barrier inhomogeneities by assuming a Gaussian distribution of barrier height due to barrier inhomogeneities that prevails at interface. This behaviour is attributed to spatial variations of the BHs. The temperature-dependent current-voltage characteristics of the SBDs have shown three Gaussian distribution giving mean BHs of

1.167, 0.652 and 0.356 eV and standard deviations 0.178, 0.087 and 0.133 V, respectively. The standard deviation decreases with increasing voltage and thus the distribution of the SBH becomes more homogenous interface. The temperature dependence of BH and ideality factor is satisfactorily explained on the basis of TE mechanism by assuming the existence of Gaussian distribution of BHs. A modified $\ln(I_0/T^2) - q^2\sigma^2/(2k^2T^2)$ vs. $(kT)^{-1}$ plot for the three temperature regions have given $\overline{\Phi}_{B0}$ and A^* as 1.173 eV and 34.750 A/cm²K² (280–400 K), 0.671 eV and 26.293 A/cm² K² (120–260 K), 0.354 eV and 10.199 A/cm² K² (40–100 K), respectively. This value of the Richardson constant of 26.293 A/cm² K² is very close to the theoretical value of 26.4 A/cm² K² for (Au/Ni)/n-GaN SBD.

References

- [1] J.S. Foresi, T.D. Moustakas. Appl. Phys. Lett., 62 (1993), p. 2859
- [2] D. Guo, M.S. Feng, R.J. Guo, F.M. Pan, C.Y. Chang. Appl. Phys. Lett., 67 (1995), p. 2657
- [3] L. Wang, M.I. Nathan, T.-H. Lim, M.A. Khan, Q. Chen. Appl. Phys. Lett., 68 (1996), p. 1267
- [4] T.U. Kampen, W. Mönch. Appl. Surf. Sci., 117 (118) (1997), p. 388
- [5] S.N. Mohammad, H. Morkoç. Prog. Quantum Electron., 20 (1996), p. 361
- [6] S.J. Pearton, J. Zolper, R.J. Shul, F. Ren. J. Appl. Phys., 86 (1999), p. 1
- [7] S. Nakamura, T. Mukai, M. Senoh. Jpn. J. Appl. Phys., 30 (1991), p. L1998
- [8] M.A. Khan, J.N. Kuznia, D.T. Olsen, M. Blasingame, A.R. Bhattaria. Appl. Phys. Lett., 63 (1993), p. 2455
- [9] J.C. Carrano, T. Li, D.L. Brown, P.A. Grudowski, C.J. Eiting, R.D. Dupuis, J.C. Campbell. Appl. Phys. Lett., 73 (1998), p. 2405
- [10] A. Teke, S. Dogan, F. Yun, M.A. Reshchikov, H. Le, X.Q. Liu, H. Morkoc, S.K. Zhang, W.B. Wang, R.R. Alfano. Solid-State Electron., 47 (2003), p. 1401
- [11] S. Dogan, S. Duman, B. Gürbulak, S. Tüzemen, H. Morkoç, Physica E 41 (2009) 646.
- [12] B. Prasanna Lakshmi, M. Siva Pratap Reddy, A. Ashok Kumar, V. Rajagopal Reddy, Curr. Appl Phys. 12 (2012) 765.
- [13] M. Siva Pratap Reddy, A. Ashok Kumar, V. Rajagopal Reddy, Thin Solid Films 519 (2011) 3844.
- [14] S. Demirezen, S. Altındal, Curr. Appl Phys. 10 (2010) 1188.
- [15] K.R. Peta, B-G Park, S-T Lee, M-D Kim, J-E Oh, Microelectron. Eng. 93 (2012) 100.
- [16] S. K. Cheung, N. W. Cheung, Appl. Phys. Lett. 49 (1986) 85.
- [17] E.H. Rhoderick, R. H. Williams, Metal-Semiconductor Contacts. Clarendon, Oxford, 1988.
- [18] X.J. Wang, L. He, J. Electron. Mater. 27 (1998) 1272.

- [19] B. Akkal, Z. Benamara, A. Boudissa, N. Bachirboudjra, M. Amrani, L. Bideux, B. Gruzza, Mater. Sci. Eng. B 55 (1998) 162.
- [20] Y. Kribes, I. Harisson, B. Tuck, T.S. Cheg, C.T. Foxon, Semicond. Sci. Technol. 12 (1997) 913.
- [21] S. Zeyrek, Ş. Altındal, H. Yüzer, M.M. Bülbül, Appl. Surf. Sci., 252 (2006) 2999
- [22] S.M. Sze Physics of Semiconductor Devices(second ed.)Willey, New York (1981)
- [23] S. Karataş, S.Altındal, A.Türüt, A.Özmen, Appl. Surf. Sci. 217 (2003) 250.
- [24] J. H. Werner, H. H. Guttler, J. Appl. Phys. 69 (1991) 1522.
- [25] A. Gümüş, A. Türüt, N. Yalçın, J. Appl. Phys. 91 (2002) 245.
- [26] S. Chand, J. Kumar, Appl. Phys. A 63 (1996) 171.
- [27] R. Hackam, P. Harrop, IEEE T. Electron Dev. ED-19 (1972) 1231-1238.
- [28] A. S. Bhuiyan, A. Martinez, D. Esteve, Thin Solid Films 161 (1988) 93-100.
- [29] M. Missous, E. H. Rhoderick, J. Appl. Phys. 69 (1991) 7142.
- [30] S. Chand, J. Kumar, Semicond. Sci. Technol. 11 (1996) 1203.
- [31] S. Zhu, R. L. Van Meirhaeghe, C. Detavernier, G. P. Ru, B. Z. Li, F. Cardon, Solid- State Commun. 112 (1999) 611.
- [32] W. Mönch, J. Vac. Sci. Technol. B 17 (1999) 1867.
- [33] T.U. Kampen, W. Mönch, Surf. Sci. 331- 333 (1995) 490.
- [34] K. Akkılıç, T. Kılıçoğlu, A. Türüt, Physica B 337 (2003) 388.
- [35] H. Dogan, N. Yıldırım, A. Türüt, M. Biber, E. Ayyıldız, C. Nuhoglu, Semicond. Sci. Technol. 21 (2006) 822.
- [36] R.T Tung, Phys. Rev. B 45 (1992) 13509. Appl. Phys. Rev. 1, 011304 (2014).
- [37] J. P Sullivan, R.T. Tung, M. R. Pinto, W. R. Graham, J. Appl. Phys. 70 (1991) 7403.
- [38] S. Chand, J. Kumar, Semicond. Sci. Technol. 10 (1995) 1680.
- [39] N. Yıldırım, K. Ejderha, A. Türüt, J. Appl. Phys. 108 (2010).
- [40] N. Yıldırım, A. Türüt, Microelectron. Eng. 86 (2009) 2270.
- [41] J. Osvald, Z. J. Horvath, Appl. Surf. Sci. 234 (2004) 349.
- [42] G. M Vanalme, R. L. Van Meirhaeghe, F. Cardon, P. Van Daele, Semicond. Sci. Technol. 14 (1999) 871.
- [43] G. M Vanalme, R. L. Van Meirhaeghe, F. Cardon, P. Van Daele, Semicond. Sci. Technol. 12 (1997) 907.
- [44] V. Kumar, L. Zhao, D. Selvanathan, and I. Adesida, J. Appl. Phys. 92, 1712 (2002).

Highlights

- 1- In this work, an attempt is made to investigate the detailed electrical properties of (Au/Ni)/*n*-GaN Schottky barrier diodes (SBDs) in a wide temperature range 40-400 K with a temperature step of 20 K by using the forward bias I-V measurements.
- 2- Barrier height (Φ_{B0}), ideality factor (n) and series resistance (R_s) of the device are extracted from the forward bias I-V measurements.
- 3- The series resistance (R_s) parameter determined from forward bias I-V characteristics using Cheung and Cheung's method.

Graphical Abstract

Forward bias semi-logarithmic I-V characteristics of (Au/Ni)/*n*-GaN SBD at various temperatures and The temperature dependence of BH for (Au/Ni)/*n*-GaN SBD obtained from the forward bias *I-V* data at various temperatures was calculated.

The temperature dependence of n for (Au/Ni)/*n*-GaN SBD obtained from the forward bias *I-V* data at various temperatures and the temperature dependence of the series resistances obtained from Cheung's method for (Au/Ni)/*n*-GaN SBD was calculated.

Richardson plots of the $\ln(I_0/T^2)$ vs. $10^3/nT$ for (Au/Ni)/*n*-GaN SBD and plot of the experimental BH vs. the n for (Au/Ni)/*n*-GaN SBD shown.

The zero-bias apparent barrier height ($\Phi_{B0}(I-V)$) vs. $1/2kT$ plot and the ideality factor ($n^{-1}-1$) vs. $1/2kT$ plot for (Au/Ni)/*n*-GaN SBD according to three Gaussian distributions shown.

Modified Richardson ($\ln(I_0/T^2) - q^2 \sigma_0^2 / 2k^2 T^2$) plot for (Au/Ni)/*n*-GaN SBD according to three Gaussian distributions of BHs was calculated.

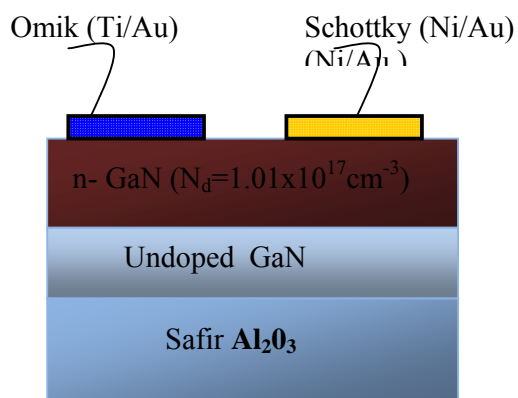


Fig. 1. Schottky contact on n-GaN

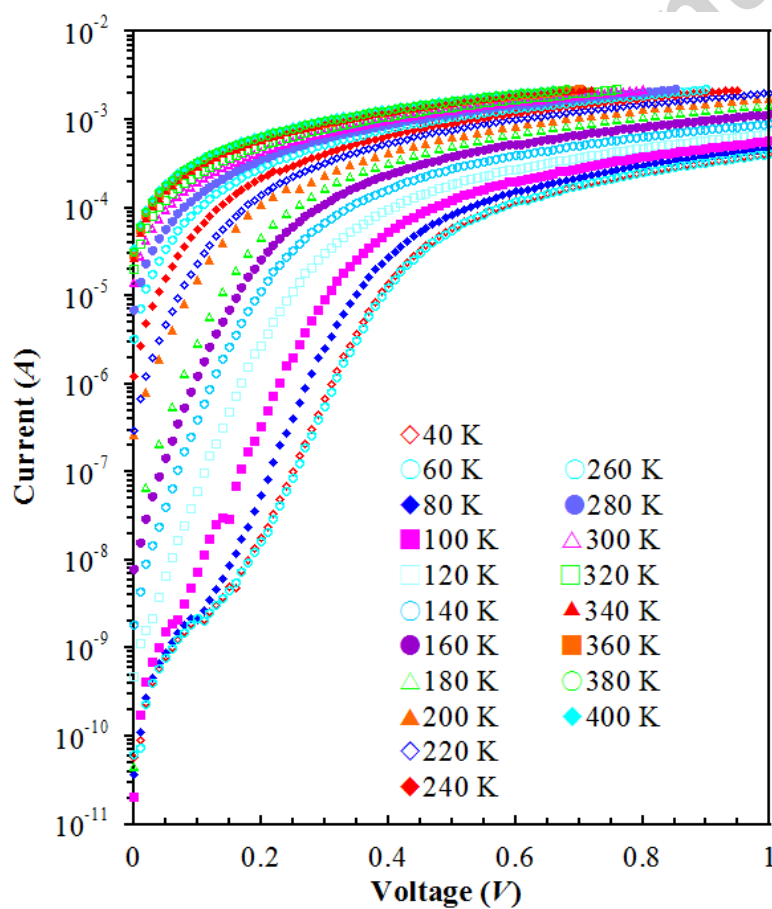


Fig. 2. Forward bias semi-logarithmic I-V characteristics of (Ni/Au)/n-GaN SBD at various temperatures.

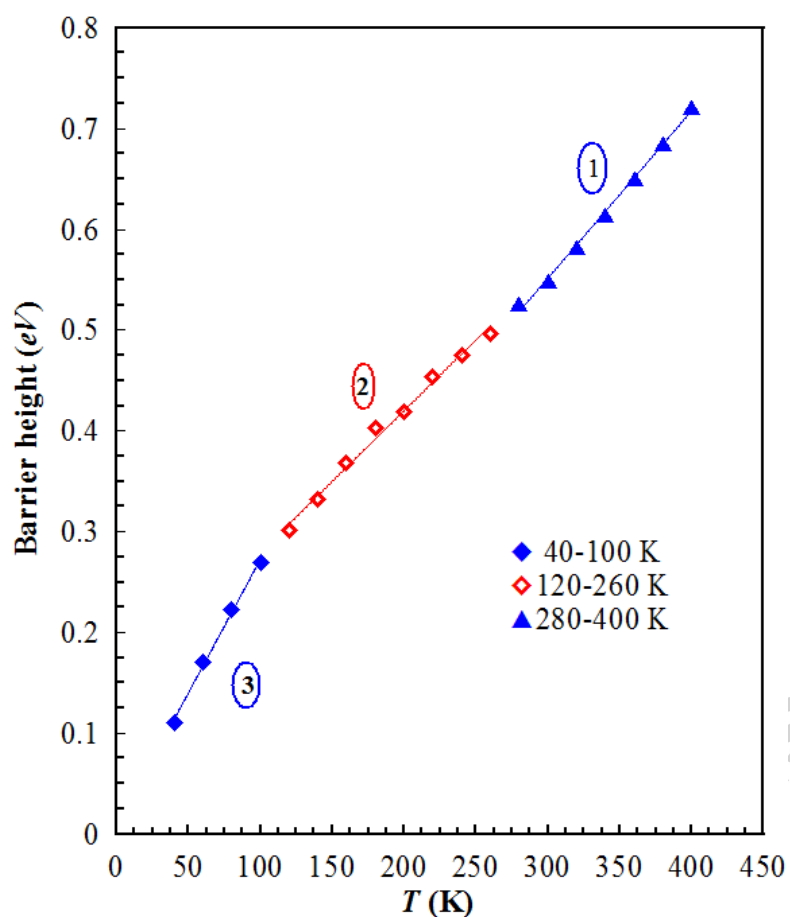


Fig. 3. The temperature dependence of BH for (Ni/Au)/n-GaN SBD obtained from the forward bias I - V data at various temperatures.

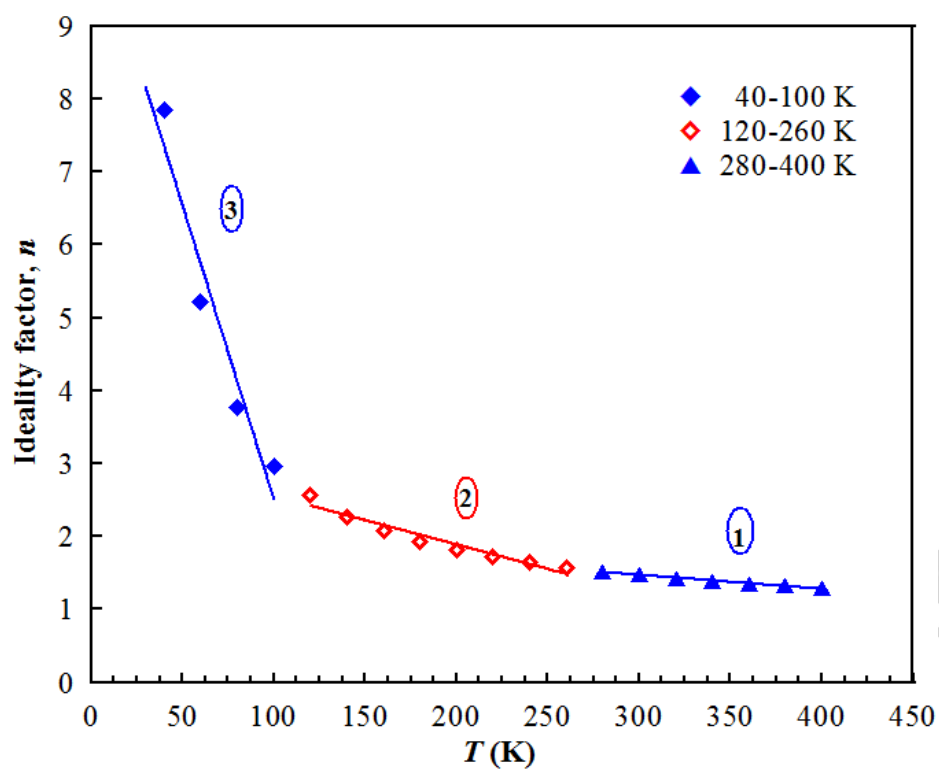


Fig. 4. The temperature dependence of n for (Ni/Au)/n-GaN SBD obtained from the forward bias I - V data at various temperatures.

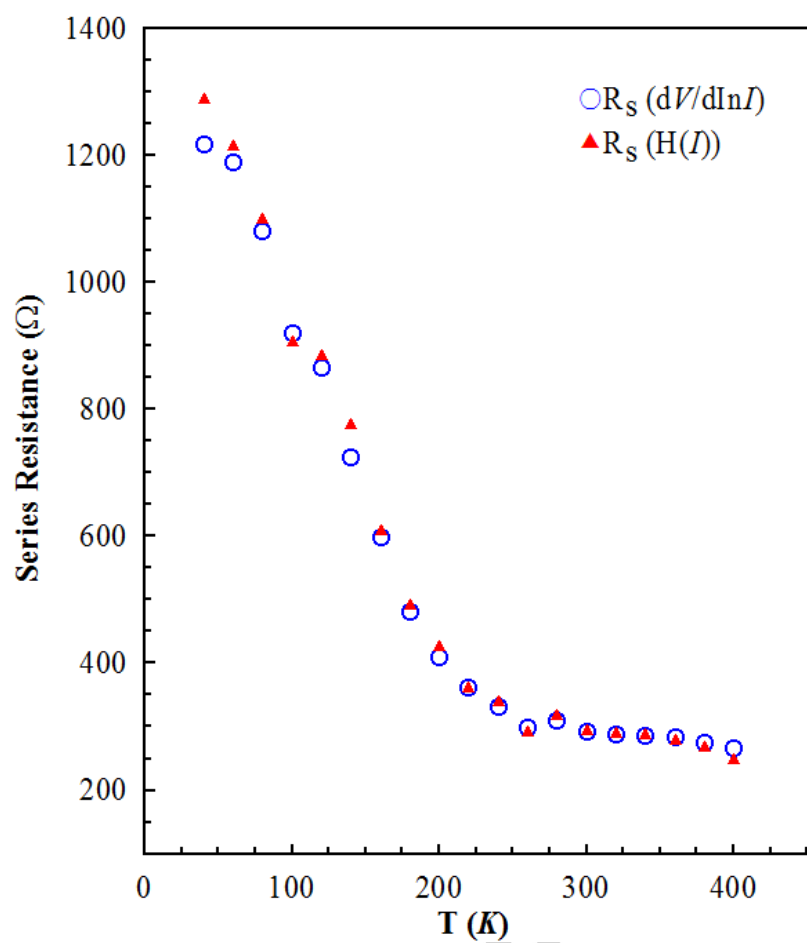


Fig.5. The temperature dependence of the series resistances obtained from Cheung's method for (Ni/Au)/n-GaN SBD.

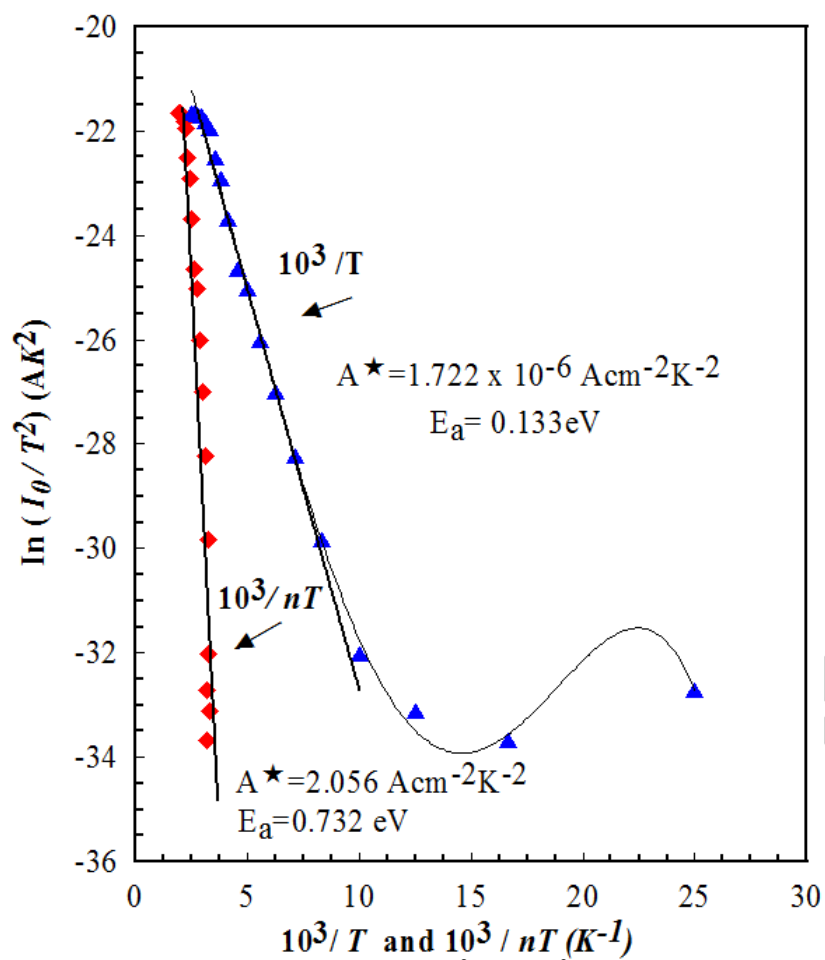


Fig.6. Richardson plots of the $\ln(I_0/T^2)$ vs. $10^3/nT$ for (Ni/Au)/n-GaN SBD.

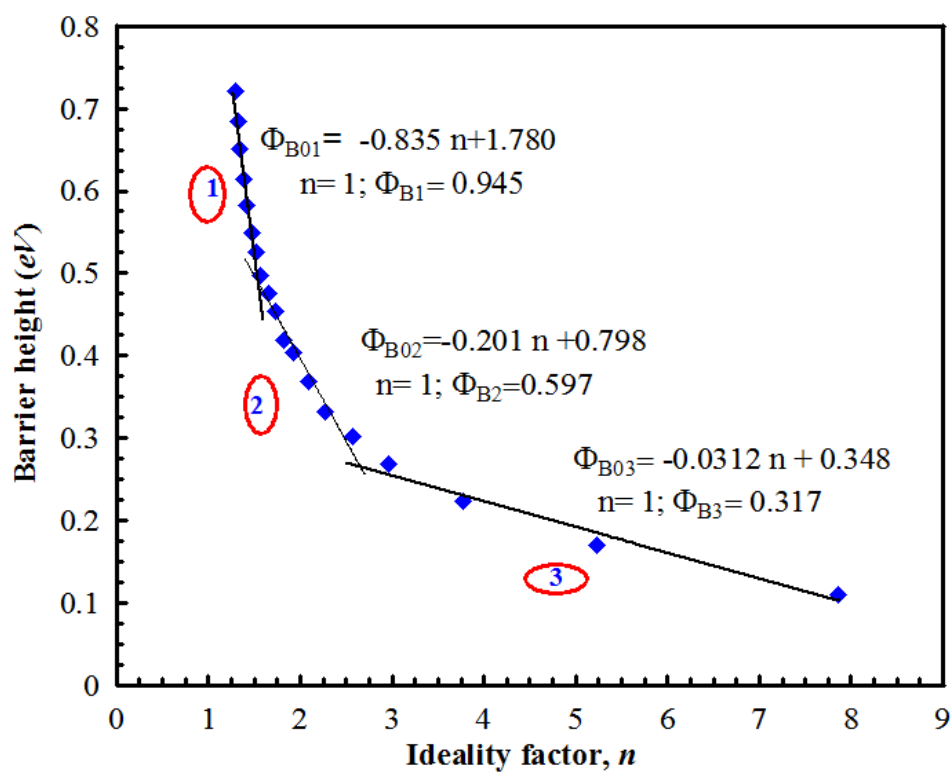
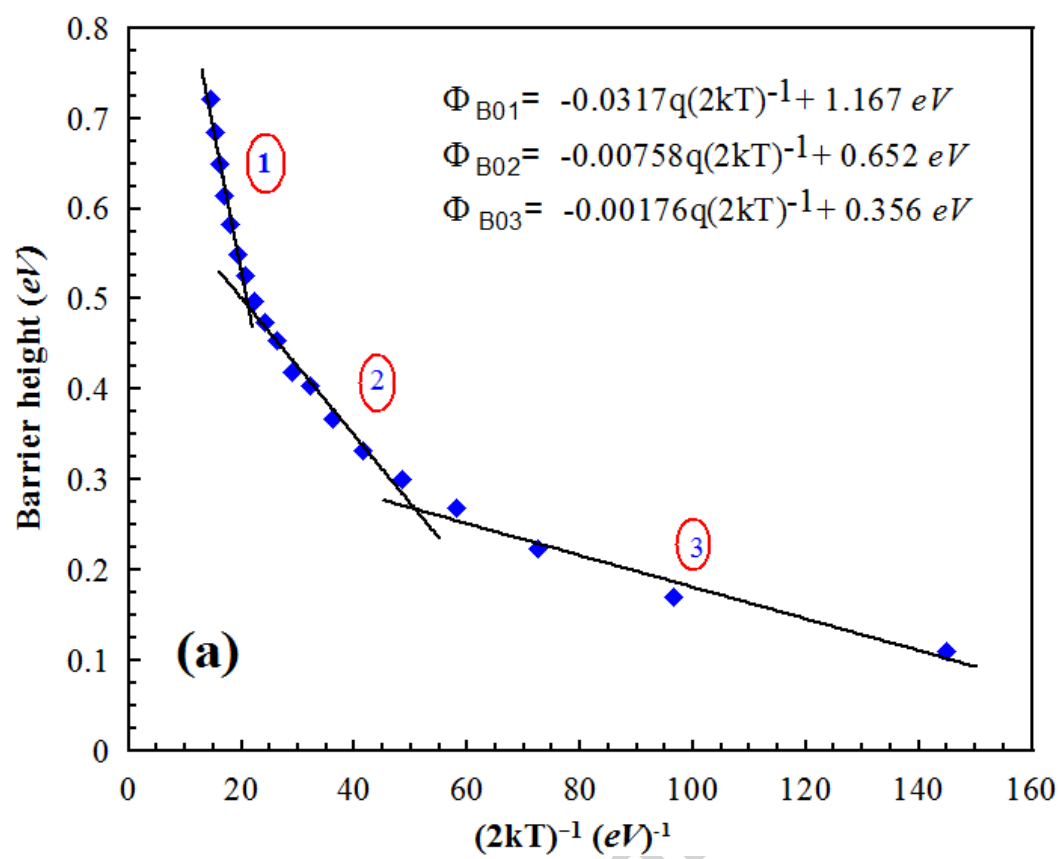


Fig.7. Plot of the experimental BH vs. the n for (Ni/Au)/ n -GaN SBD.



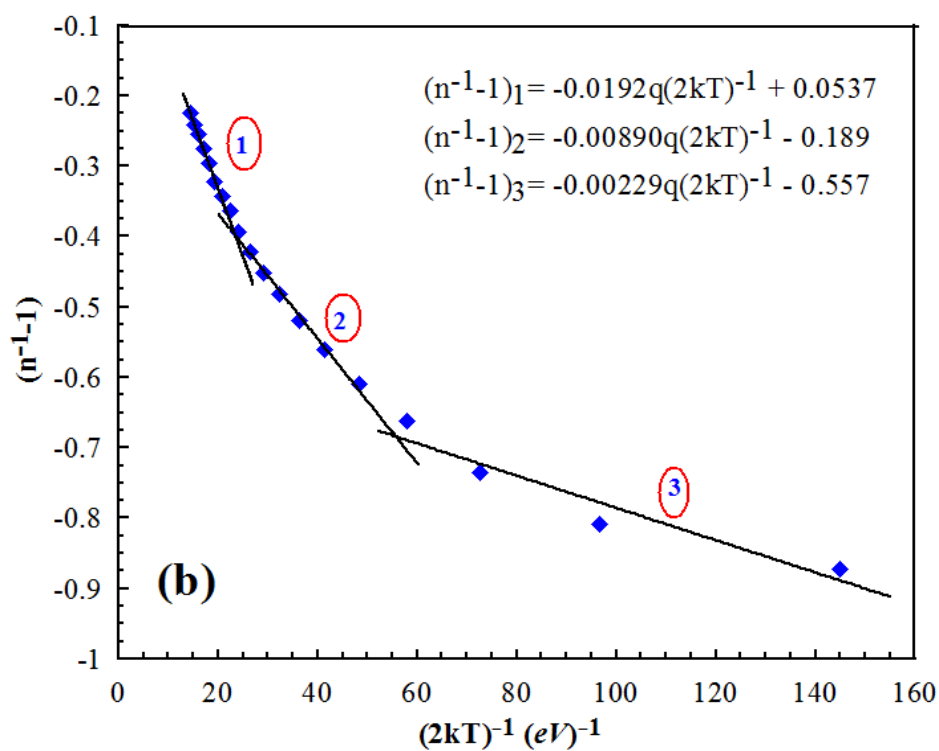


Fig. 8. (a) The zero-bias apparent barrier height ($\Phi_{B0}(I-V)$) vs. $1/2kT$ plot, (b) the ideality factor ($n^{-1}-1$) vs. $1/2kT$ plot for (Ni/Au)/n-GaN SBD according to the three Gaussian distribution.

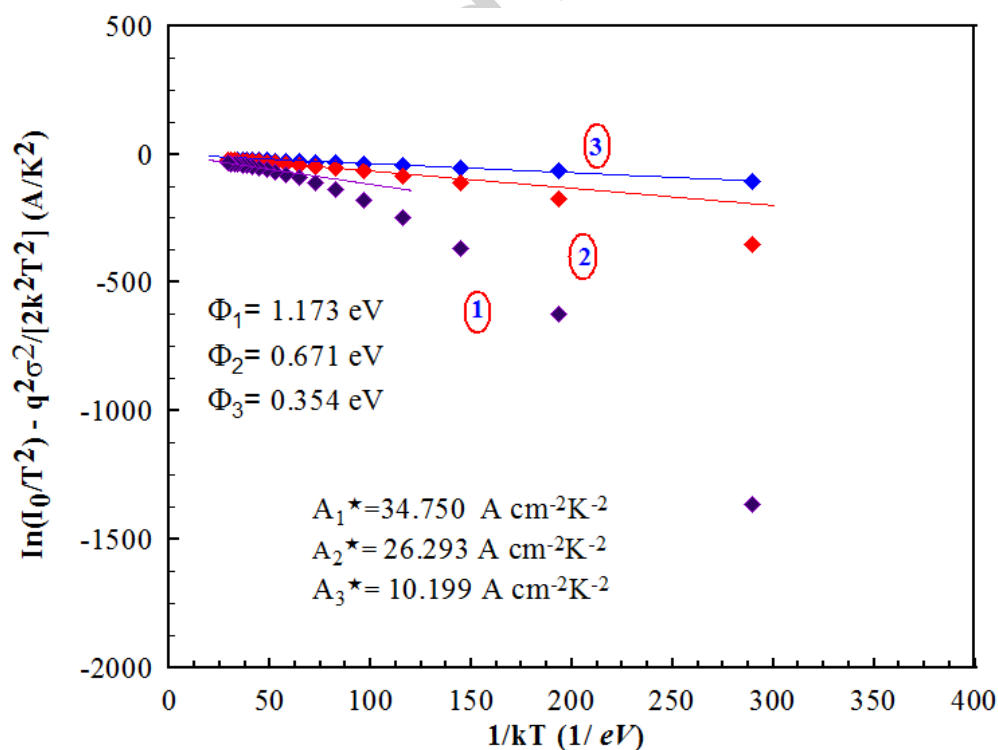


Fig.9. Modified Richardson ($\ln(I_0/T^2) - q^2 \sigma_0^2/2k^2T^2$) plot for (Ni/Au)/n-GaN SBD according to the three Gaussian distributions of the barrier height.

Table 1. Temperature dependent values of various parameters determined from forward bias I-V characteristics of (Ni/Au)/n-GaN SBD.

T(K)	$n_{(I-V)}$	$\Phi_{Bo(I-V)} (eV)$	$\Phi_{Bo(H-I)} (eV)$	$R_{s(dV/d(\ln I))} (\Omega)$	$R_{s(H-I)} (\Omega)$
40	7.850	0.110	0.104	1217.76	1287.61
60	5.225	0.170	0.143	1188.56	1213.88
80	3.777	0.223	0.187	1079.33	1098.56
100	2.959	0.269	0.205	919.53	904.60
120	2.556	0.301	0.264	866.02	882.81
140	2.273	0.332	0.299	724.42	733.53
160	2.085	0.368	0.340	598.55	607.80
180	1.925	0.403	0.374	480.44	489.18
200	1.823	0.419	0.388	409.10	425.20
220	1.727	0.454	0.403	361.25	360.06
240	1.649	0.475	0.439	331.13	338.26
260	1.573	0.497	0.433	298.58	289.57
280	1.520	0.526	0.481	310.92	317.32
300	1.476	0.549	0.488	292.95	291.70
320	1.419	0.582	0.519	287.68	289.02
340	1.384	0.614	0.543	286.90	285.11
360	1.340	0.650	0.572	282.97	278.23
380	1.321	0.685	0.599	274.82	266.28
400	1.289	0.721	0.638	267.30	247.57

Table 1

T(K)	$n_{(I-V)}$	$\Phi_{Bo(I-V)} (eV)$	$\Phi_{Bo(H-I)} (eV)$	$R_{s(dV/d(\ln I))} (\Omega)$	$R_{s(H-I)} (\Omega)$
40	7.850	0.110	0.104	1217.76	1287.61
60	5.225	0.170	0.143	1188.56	1213.88
80	3.777	0.223	0.187	1079.33	1098.56
100	2.959	0.269	0.205	919.53	904.60
120	2.556	0.301	0.264	866.02	882.81
140	2.273	0.332	0.299	724.42	733.53
160	2.085	0.368	0.340	598.55	607.80
180	1.925	0.403	0.374	480.44	489.18
200	1.823	0.419	0.388	409.10	425.20
220	1.727	0.454	0.403	361.25	360.06
240	1.649	0.475	0.439	331.13	338.26
260	1.573	0.497	0.433	298.58	289.57
280	1.520	0.526	0.481	310.92	317.32
300	1.476	0.549	0.488	292.95	291.70
320	1.419	0.582	0.519	287.68	289.02
340	1.384	0.614	0.543	286.90	285.11
360	1.340	0.650	0.572	282.97	278.23
380	1.321	0.685	0.599	274.82	266.28
400	1.289	0.721	0.638	267.30	247.57

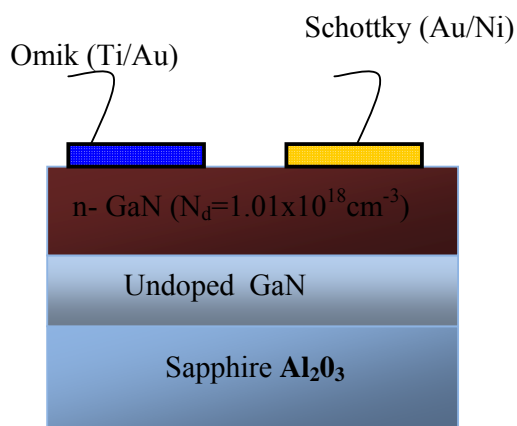


Fig. 1. Schottky contact on n-GaN

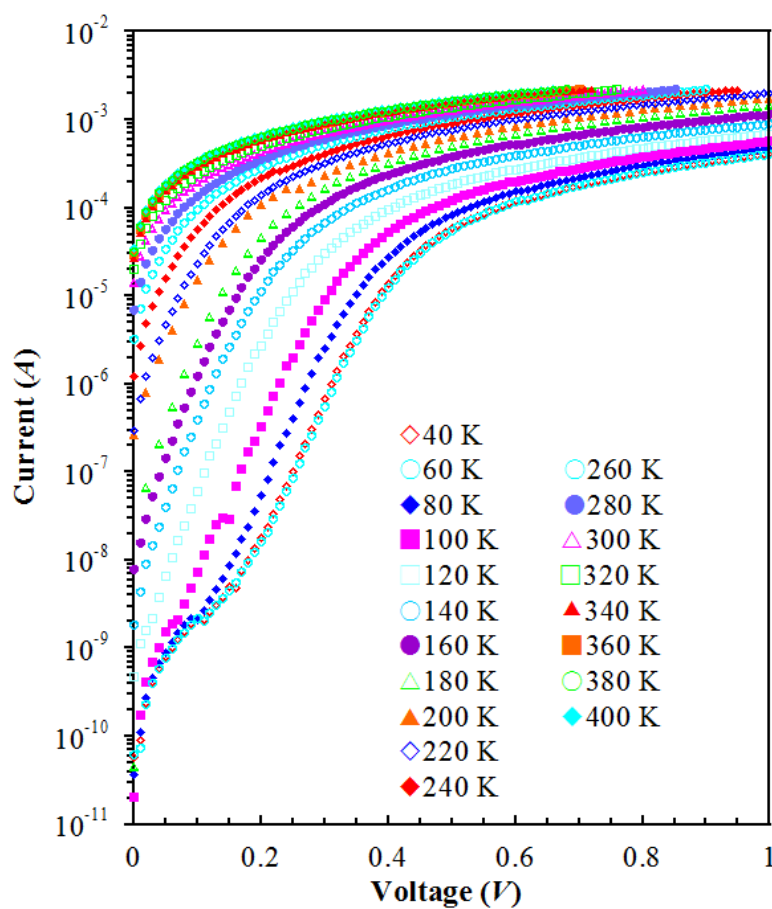


Fig. 2. Forward bias semi-logarithmic I-V characteristics of (Au/Ni)/n-GaN SBD at various temperatures.

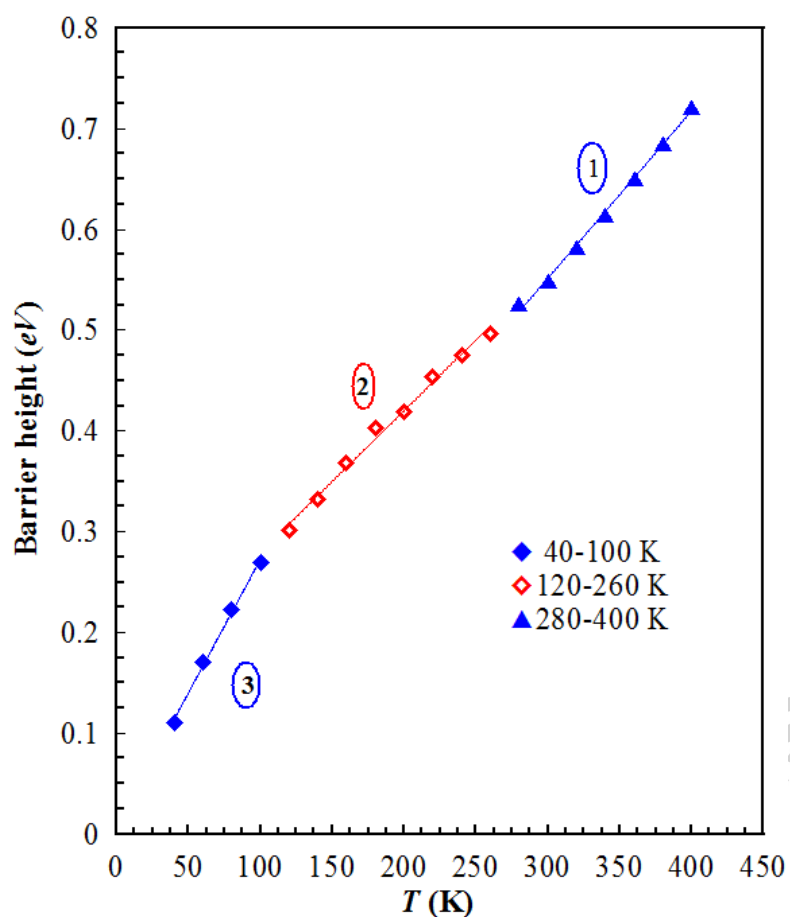


Fig. 3. The temperature dependence of BH for (Au/Ni)/n-GaN SBD obtained from the forward bias I - V data at various temperatures.

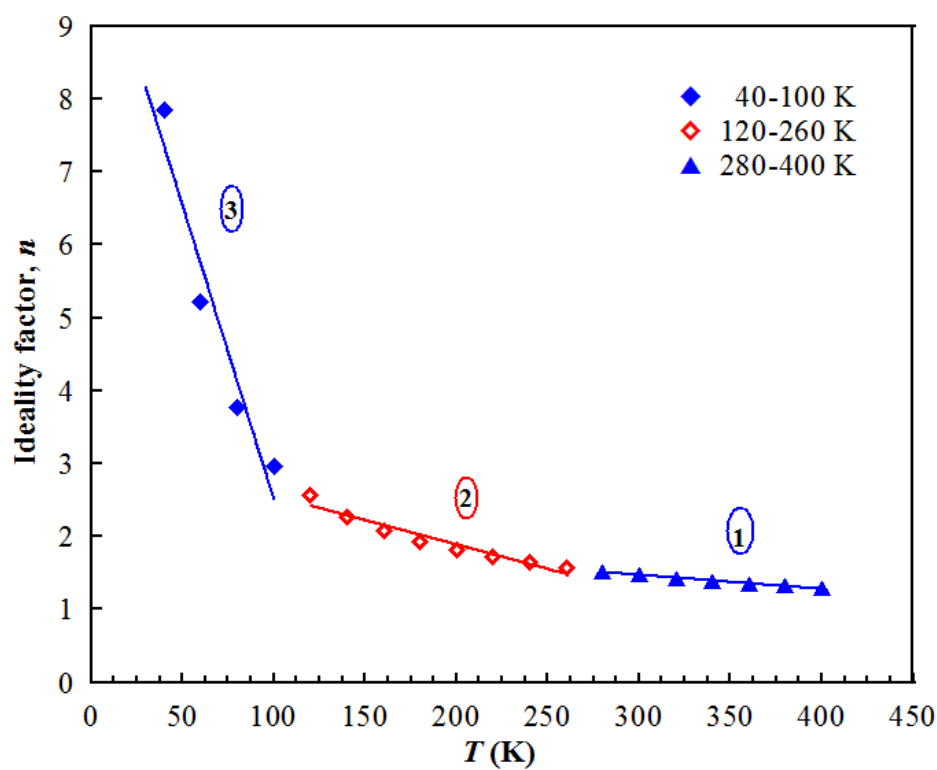


Fig. 4. The temperature dependence of n for (Au/Ni)/n-GaN SBD obtained from the forward bias I - V data at various temperatures.

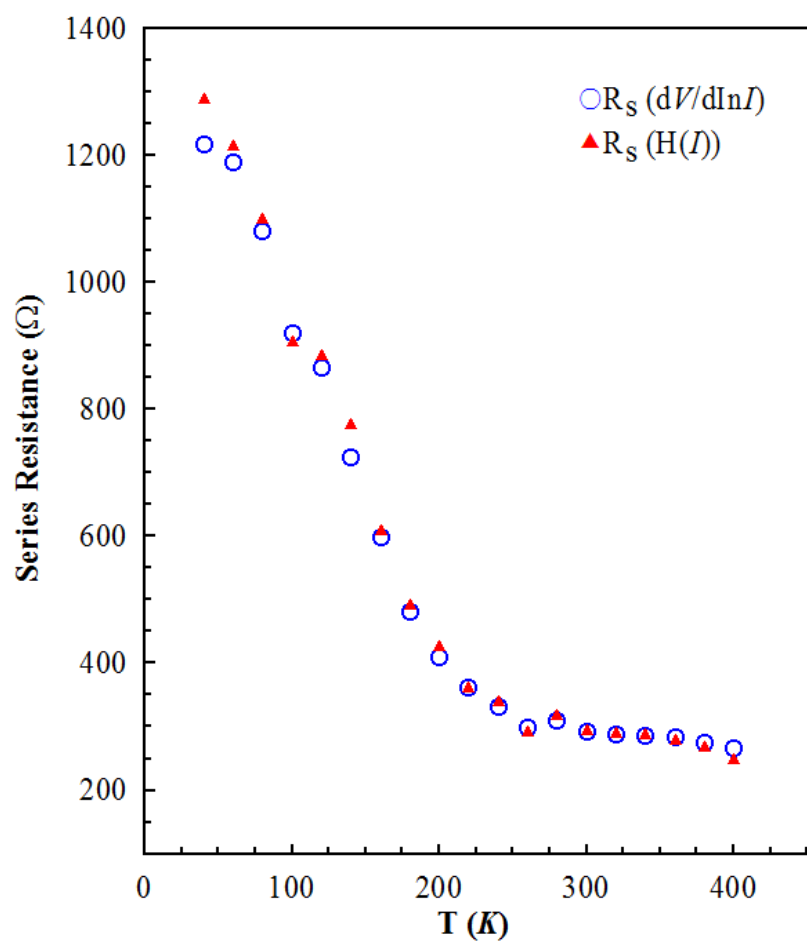


Fig.5. The temperature dependence of the series resistances obtained from Cheung's method for (Au/Ni)/n-GaN SBD.

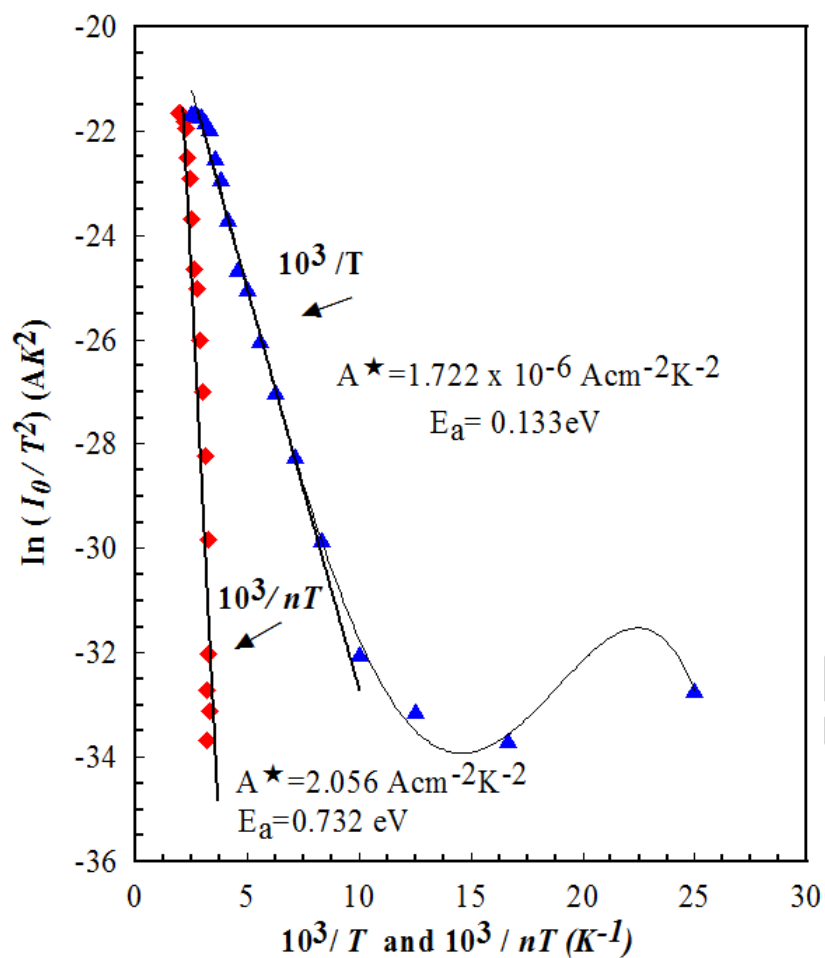


Fig.6. Richardson plots of the $\ln(I_0/T^2)$ vs. $10^3/nT$ for (Au/Ni)/n-GaN SBD.

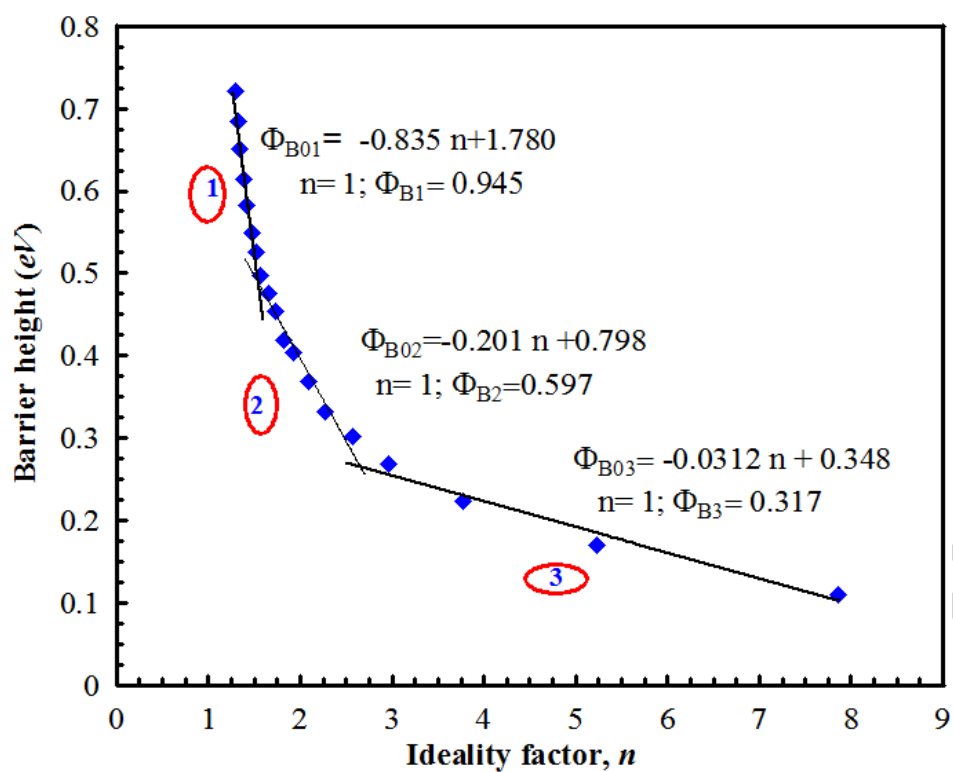
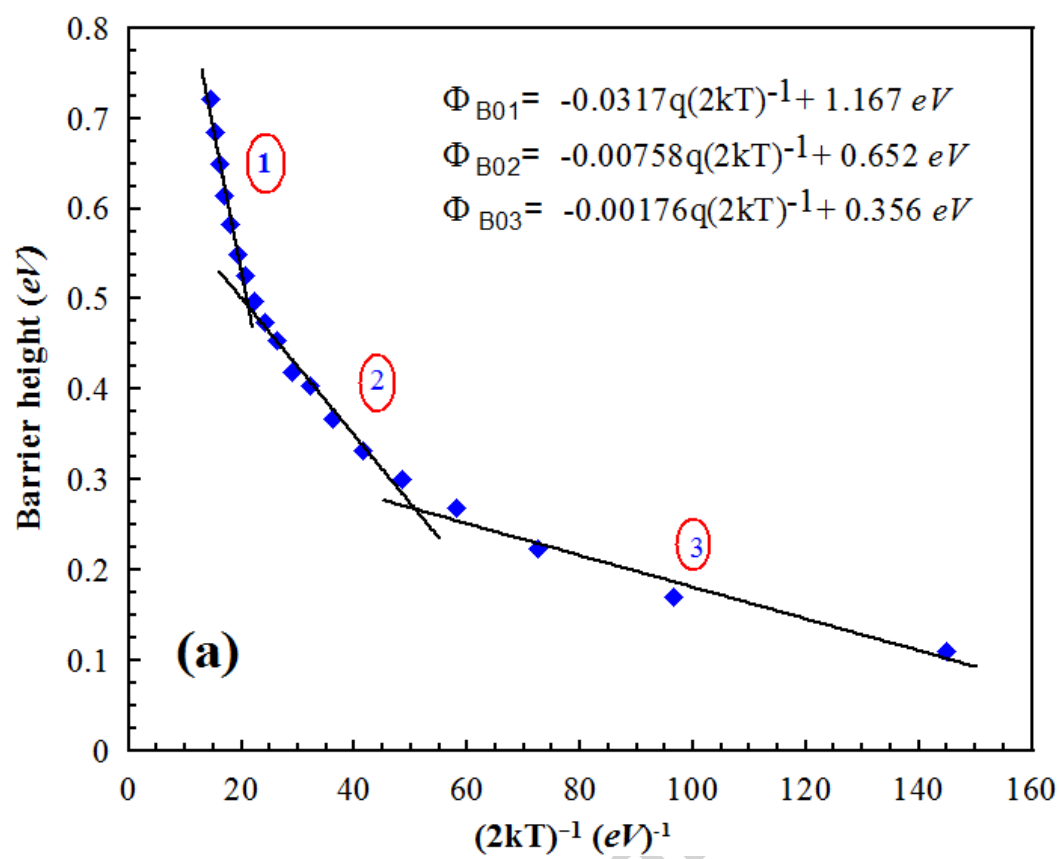


Fig.7. Plot of the experimental BH vs. the n for (Au/Ni)/ n -GaN SBD.



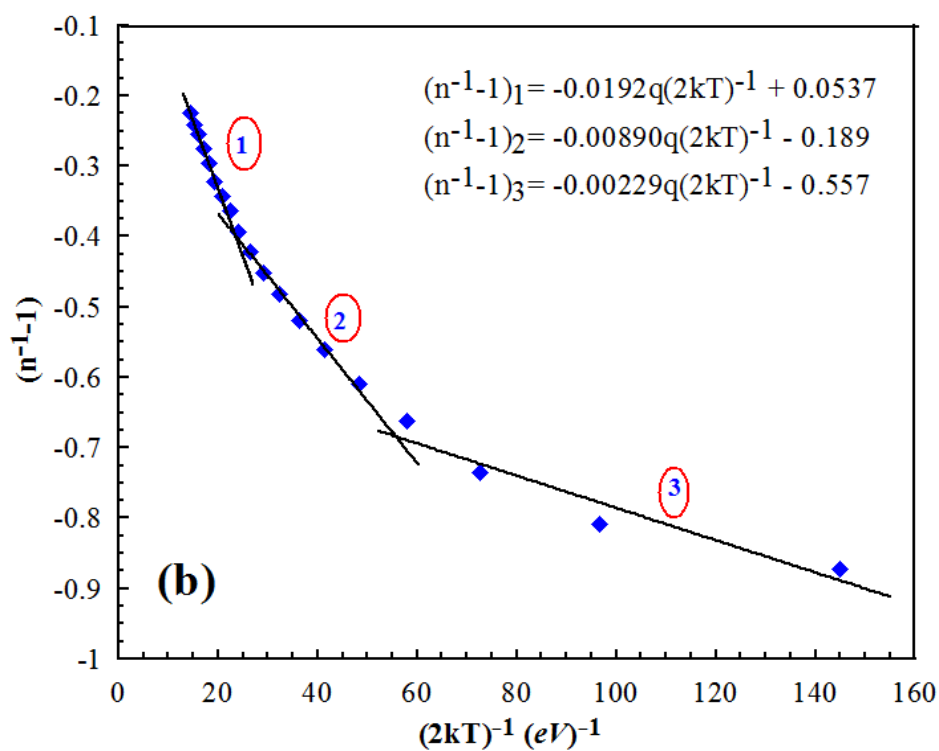


Fig. 8. (a) The zero-bias apparent barrier height ($\Phi_{B0}(I-V)$) vs. $1/2kT$ plot, (b) the ideality factor ($n^{-1}-1$) vs. $1/2kT$ plot for (Au/Ni)/n-GaN SBD according to the three Gaussian distribution.

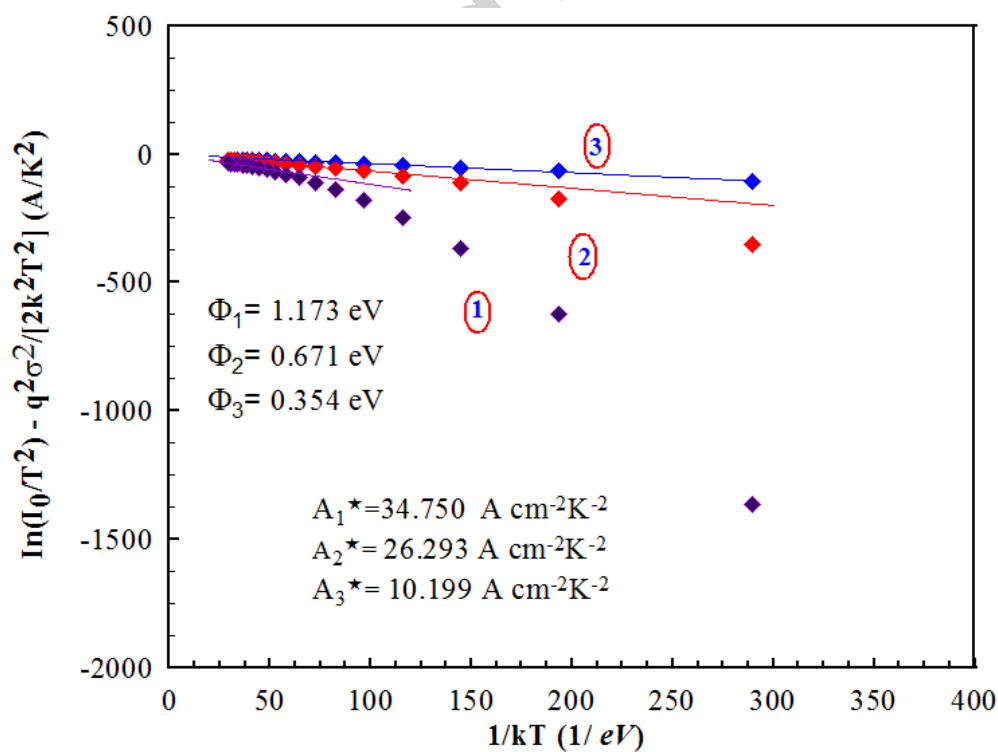


Fig.9. Modified Richardson ($\ln(I_0/T^2) - q^2 \Phi_B / 2k^2 T^2$) plot for (Au/Ni)/*n*-GaN SBD according to the three Gaussian distributions of the barrier height.

Highlights

- 1- In this work, an attempt is made to investigate the detailed electrical properties of (Au/Ni)/*n*-GaN Schottky barrier diodes (SBDs) in a wide temperature range 40-400 K with a temperature step of 20 K by using the forward bias I-V measurements.
- 2- Barrier height (Φ_{B0}), ideality factor (*n*) and series resistance (R_s) of the device are extracted from the forward bias I-V measurements.
- 3- The series resistance (R_s) parameter determined from forward bias I-V characteristics using Cheung and Cheung's method.